Abdominal Radiology (2019) 44:1261–1268
https://doi.org/10.1007/s00261-019-01956-x

CASE REPORT

MRI features of mucinous adenocarcinoma of the prostate: report of four cases

Kaori Yamada[1] · Nana Kozawa[2] · Hitomi Nagano[2] · Masato Fujita[1] · Kei Yamada[2]

Published online: 27 February 2019

Abstract

Case reports We report four patients with mucinous adenocarcinoma of the prostate, focusing on their magnetic resonance imaging (MRI) findings. The lesions appeared hyperintense on T2-weighted images (T2WI) in all four patients. In the two patients in whom the tumors were confined to the peripheral zone (PZ), the lesions were isointense to the surrounding normal PZ, making them difficult to identify. In all three patients who underwent diffusion-weighted imaging ($b = 1000$), the lesions appeared hyperintense but visually there was little or no decrease in the apparent diffusion coefficient (ADC), with ADC values of 1.02, 1.39, and 1.66×10^{-3} mm^2/s, respectively. In the three patients who underwent a dynamic contrast-enhanced MR study, early enhancement was evident in two (partial in one), and gradually increasing enhancement in one.

Conclusion In the four cases in this instance, MRI findings of mucinous adenocarcinoma were very different from the appearance of non-mucinous adenocarcinoma. It is suggested that the conventional interpretation method of MRI for prostate cancer is not suitable for mucinous adenocarcinoma. Those who interpret prostate MRI should be aware of this rare and unique subtype of prostate cancer.

Keywords Prostate cancer · Mucinous adenocarcinoma · MRI · PI-RADS

Introduction

Mucinous adenocarcinoma of the prostate is classified as a rare subtype of acinar adenocarcinoma and is defined as adenocarcinoma in which at least 25% of the resected specimen consists of extracellular mucin [1]. It accounts for approximately 0.4% of all prostate cancers [2]. Its imaging findings have rarely been reported, with only a small number of published case reports describing a single case, or at most a few cases. According to these reports, unlike usual adenocarcinoma, mucinous adenocarcinoma characteristically appears hyperintense on magnetic resonance imaging (MRI) T2-weighted images (T2WI), reflecting the presence of large amounts of mucin; it may therefore be difficult to diagnose by MRI if it occurs in the peripheral zone (PZ), which also appears hyperintense on T2WI [3, 4]. No comprehensive report of diffusion-weighted imaging (DWI) or dynamic contrast-enhanced MRI (DCE-MRI) findings has been published.

We report our experience of four cases of mucinous adenocarcinoma of the prostate, focusing on their MRI findings, including DWI and DCE-MRI, and compare them with pathological findings. We also explore how imaging findings in mucinous adenocarcinoma differ from those in common prostate adenocarcinoma and the possibility of pitfalls in interpretation based on the Prostate Imaging Reporting and Data System version 2 (PI-RADS v2) [5].

Case reports

Case 1

A 69-year-old man showed a slightly elevated prostate-specific antigen (PSA) level of 4.12 ng/mL at a health check-up. His physical examination, including digital rectal examination (DRE), was normal. His past medical history was

✉ Kaori Yamada
b97b36@koto.kpu-m.ac.jp

[1] Department of Diagnostic Radiology, Kyoto Second Red Cross Hospital, 355-5 Haruobi-cho, Kamigyo-ku, Kyoto 602-8026, Japan

[2] Department of Radiology, Kyoto Prefectural University of Medicine, 465 Kajii-cho, Kamigyo-ku, Kyoto 602-8566, Japan

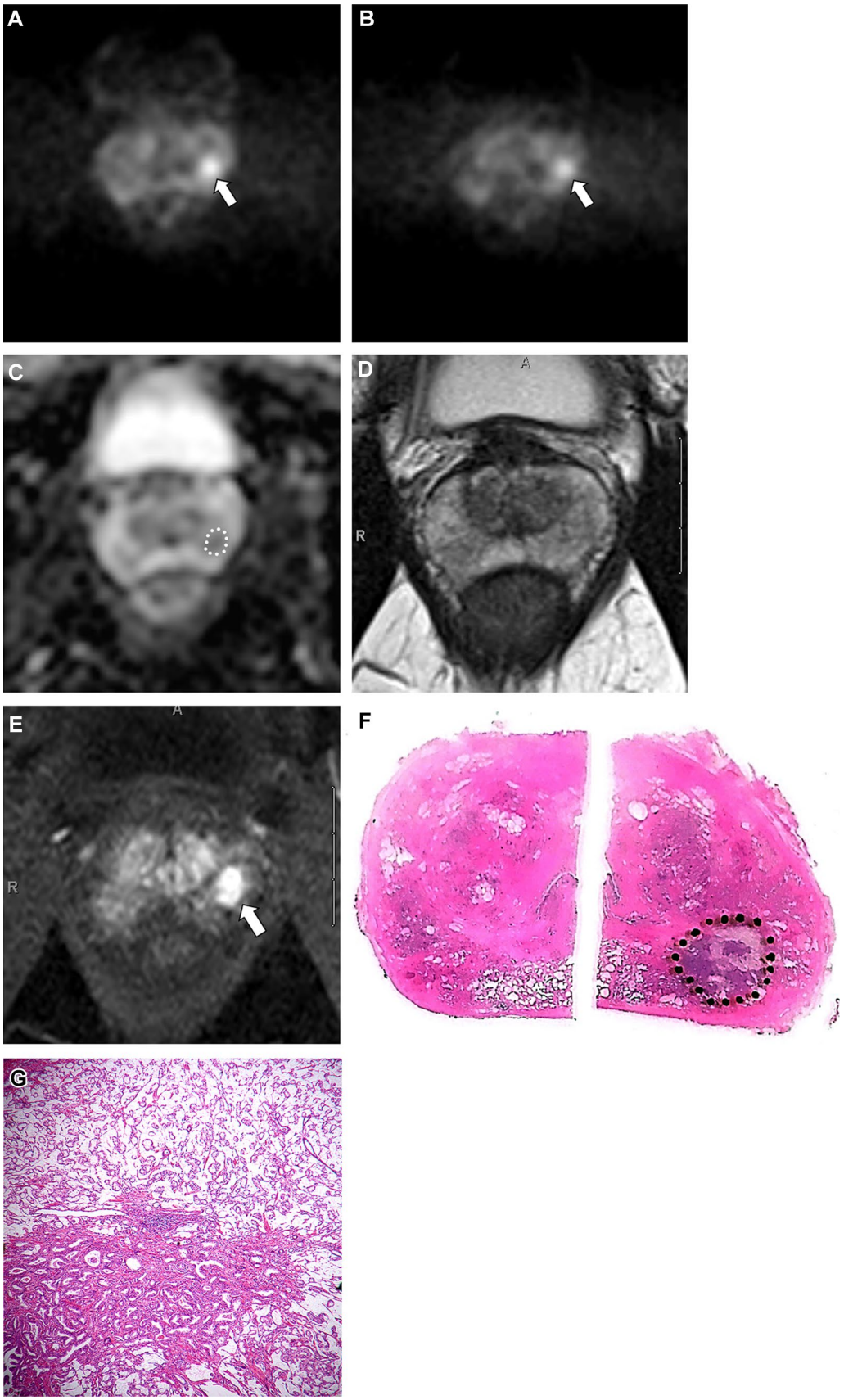
A
B
C
D
A
R
E
A
R
F
G

◂**Fig. 1** Case1: an asymptomatic 69-year-old man with a slightly elevated PSA level. **a** On diffusion-weighted images ($b=1000$), a well-demarcated nodular hyperintensity was observed in the left PZ. **b** On high b-value diffusion-weighted images ($b=1500$), the lesion still appeared as a strongly hyperintense nodule. **c** The apparent diffusion coefficient was 1.02×10^{-3} mm^2/s, only slightly lower than that of the surrounding tissue (outline). **d** On T2-weighted images, the lesion was isointense to the surrounding normal PZ and was could not be distinguished. **e** In dynamic contrast-enhanced MRI, intense early enhancement was observed in the lesion in the left PZ. **f** Hematoxylin and eosin staining of a section of the gross specimen revealed a tumor in the left PZ of the prostate (outlined). **g** Microscopy (original ×40) revealed a mixture of regions with large and small amounts of extracellular mucin

unremarkable. Prostate MRI was performed. DWI ($b=1000$, 1500) showed a well-demarcated, nodular hyperintense area in the left PZ (Fig. 1a, b), but ADC was only slightly decreased (1.02×10^{-3} mm^2/s) (Fig. 1c). On T2WI it was isointense with the surrounding normal PZ and was difficult to distinguish (Fig. 1d). In the DCE-MRI study, intense early enhancement was observed in the lesion (Fig. 1e). PI-RADS v2 defines a PZ lesion of "focal mildly/moderately hypointense on ADC and isointense/mildly hyperintense on high b-value DWI" as Category 3 and that of "focal markedly hypointense on ADC and markedly hyperintense on high b-value DWI; < 1.5 cm in greatest dimension" as Category 4 [5]. However, in this case, the lesion appeared mildly hypointense on ADC but markedly hyperintense on DWI, thus it did not fit any category. Prostate biopsy performed 58 days after the MRI showed adenocarcinoma with mucinous features with Gleason score 8 (4 + 4) in the left PZ. Radical prostatectomy was performed 126 days after the MRI assuming the diagnosis of clinical T2aN0M0 prostate cancer. Postoperative pathology revealed Gleason score 7 (4 + 3) mucinous adenocarcinoma of 1.0 × 0.8 cm in the left PZ with a stage of T2a (Fig. 1f, g). His follow-up is ongoing without any signs of recurrence for 40 months.

Case 2

A 73-year-old man visited our hospital for a high PSA (5.67 ng/mL) identified at a health check-up. His past medical history was unremarkable. His physical examination, including DRE, was normal. Prostate MRI revealed a slightly hyperintense nodule involving both lobes on the ventral side of the transition zone (TZ) on DWI ($b=1000$) (Fig. 2a). High b-value DWI (b = 2000) showed decreased signal in both the lesion and the surrounding prostate tissue; the contrast was diminished compared with that of $b=1000$ (Fig. 2b). ADC was not decreased compared with the surrounding TZ (1.39×10^{-3} mm^2/s) (Fig. 2c). On T2WI, the lesion showed a thin capsule-like rim and was hyperintense in its ventral portion and hypointense in its dorsal portion (Fig. 2d). Faint early enhancement was seen in the DCE-MRI study, mainly in the area that appeared hypointense on T2WI (Fig. 2e). The TZ lesion fit the "circumscribed heterogeneous encapsulated nodule on T2WI" description, and was classified as PI-RADS category 2. Prostate biopsy performed 35 days after MRI revealed Gleason score 8 (4 + 4) adenocarcinoma with mucinous features in the left apex. Radical prostatectomy was performed 96 days after MRI assuming the diagnosis of clinical T2cN0M0 prostate cancer. Postoperative pathology revealed a Gleason score 7 (3 + 4) mucinous adenocarcinoma 1.8 × 0.7 cm involving the anterior TZ of both lobes with a stage of T2c (Fig. 2f, g). There has been no sign of recurrence in his follow-up of 57 months.

Case 3

A 75-year-old man presenting with dysuria had been diagnosed with benign prostatic hyperplasia (BPH) in another clinic and took medications. He was also under treatment for hypertension and hypertrophic cardiomyopathy. However, urinary retention had recurred repeatedly and he was referred to our hospital for transurethral resection of the prostate (TURP). His PSA level was not elevated (0.503 ng/mL). On DRE, the prostate was enlarged, and a hard mass was palpable in both lobes. TURP was performed and most of the resected specimens were involved by tumor with large amounts of extracellular mucin (Fig. 3a). Microscopically, numerous mucous nodules (mucin lakes) were found, with tumor cells with signet ring cells floating therein (Fig. 3b). Other primary or metastatic lesions were ruled out by gastrointestinal endoscopy and 18F-fluorodeoxyglucose positron emission tomography/computed tomography, and it was diagnosed as mucinous adenocarcinoma of prostate origin. MRI performed 14 days after TURP revealed the entire prostate to be occupied by a large mass bulging outside the capsule. The lesion appeared strongly hyperintense on DWI ($b=1000$) (Fig. 3c), but the signal decreased on high b-value DWI ($b=1500$) (Fig. 3d). The mean ADC of the mass was as high as 1.66×10^{-3} mm^2/s (Fig. 3e) and the lesion also appeared slightly hyperintense on T2WI (Fig. 3f); the hyperintensity on DWI was considered to be caused by T2 shine-through effect. This lesion showed gradually increasing contrast enhancement on DCE-MRI (Fig. 3g). There was no applicable category in PI-RADS v2 for this mass. The tumor invaded the seminal vesicles and the bladder neck, but metastasis was not recognized and the clinical stage was determined as T4N0M0. Despite multidisciplinary therapy including hormonal therapy, chemotherapy, and interstitial brachytherapy, the disease progressed and palliative care was introduced.

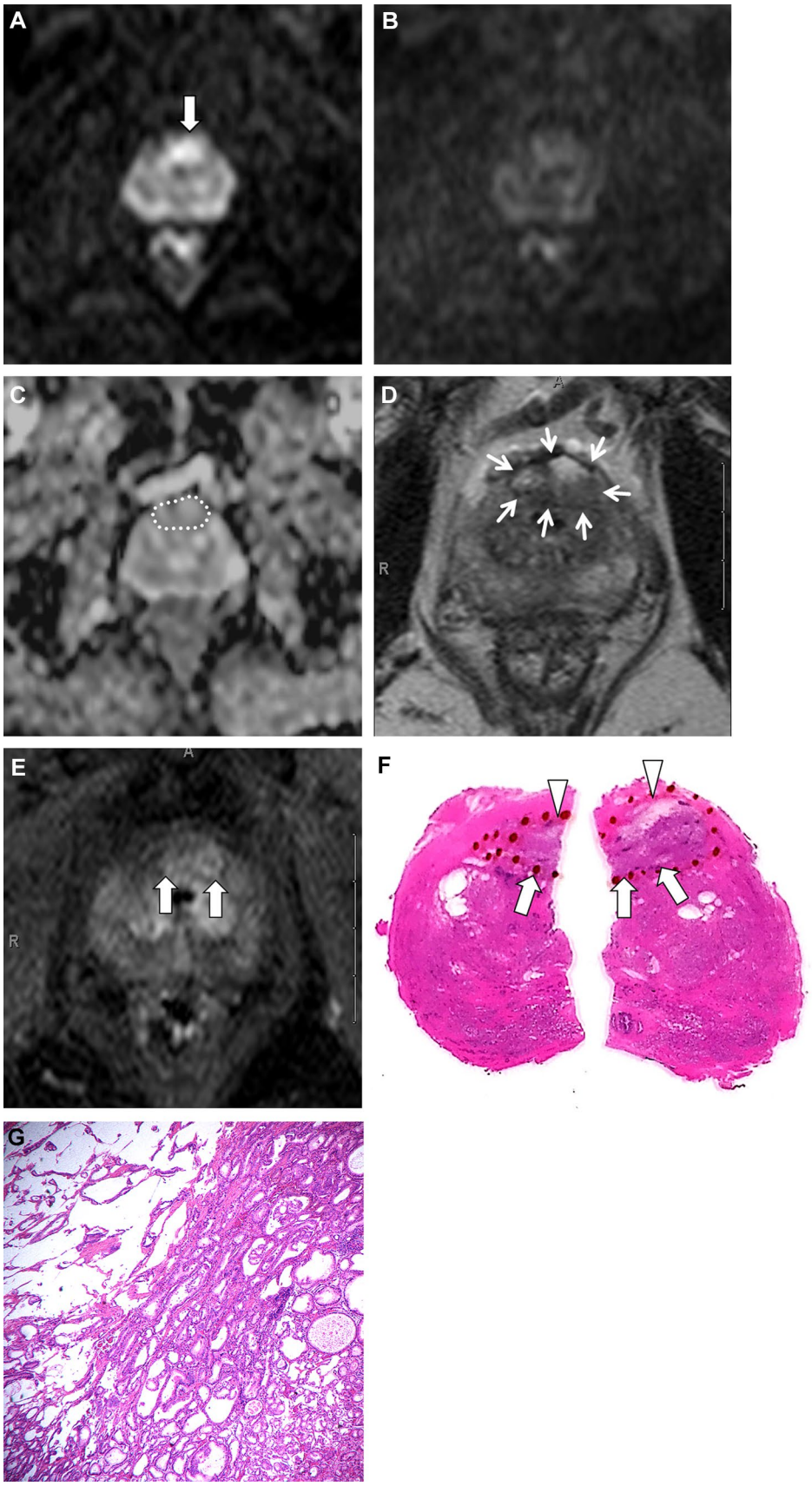

Fig. 2 Case 2: a 73-year-old man with high PSA (5.67 ng/mL). **a** Diffusion-weighted imaging (b = 1000) showed slightly hyperintense nodule in the anterior TZ (arrow). **b** On high b-value diffusion-weighted images ($b = 2000$), a part of the lesion still showed indistinct hyperintensities but both signals of the lesion and surrounding prostate tissue decreased and the contrast between the lesion and surrounding tissue diminished compared with that of diffusion-weighted imaging with $b = 1000$. **c** There was no decrease in apparent diffusion coefficient compared with the surrounding TZ (1.39×10^{-3} mm^2/s). **d** On T2-weighted images, the lesion had a thin capsule-like rim (small arrows), and hyperintensities in the ventral portion and hypointensities of the dorsal portion of the lesion were evident. **e** Faint early enhancement was observed on dynamic contrast-enhanced MRI, mainly in the area that appeared hypointense on T2-weighted images (arrows). **f** Hematoxylin and eosin staining of a gross specimen of the resected prostate revealed a tumor extending across both lobes on the ventral side of the prostate (outlined). Cell density was comparatively high in the dorsal part of the lesion (arrows), but the ventral part appeared more translucent because of its high extracellular mucin content (arrowheads). **g** Microscopic examination (hematoxylin and eosin staining, original ×40) also revealed regions with low cell density due to the high extracellular mucin content and regions of comparatively high cell density

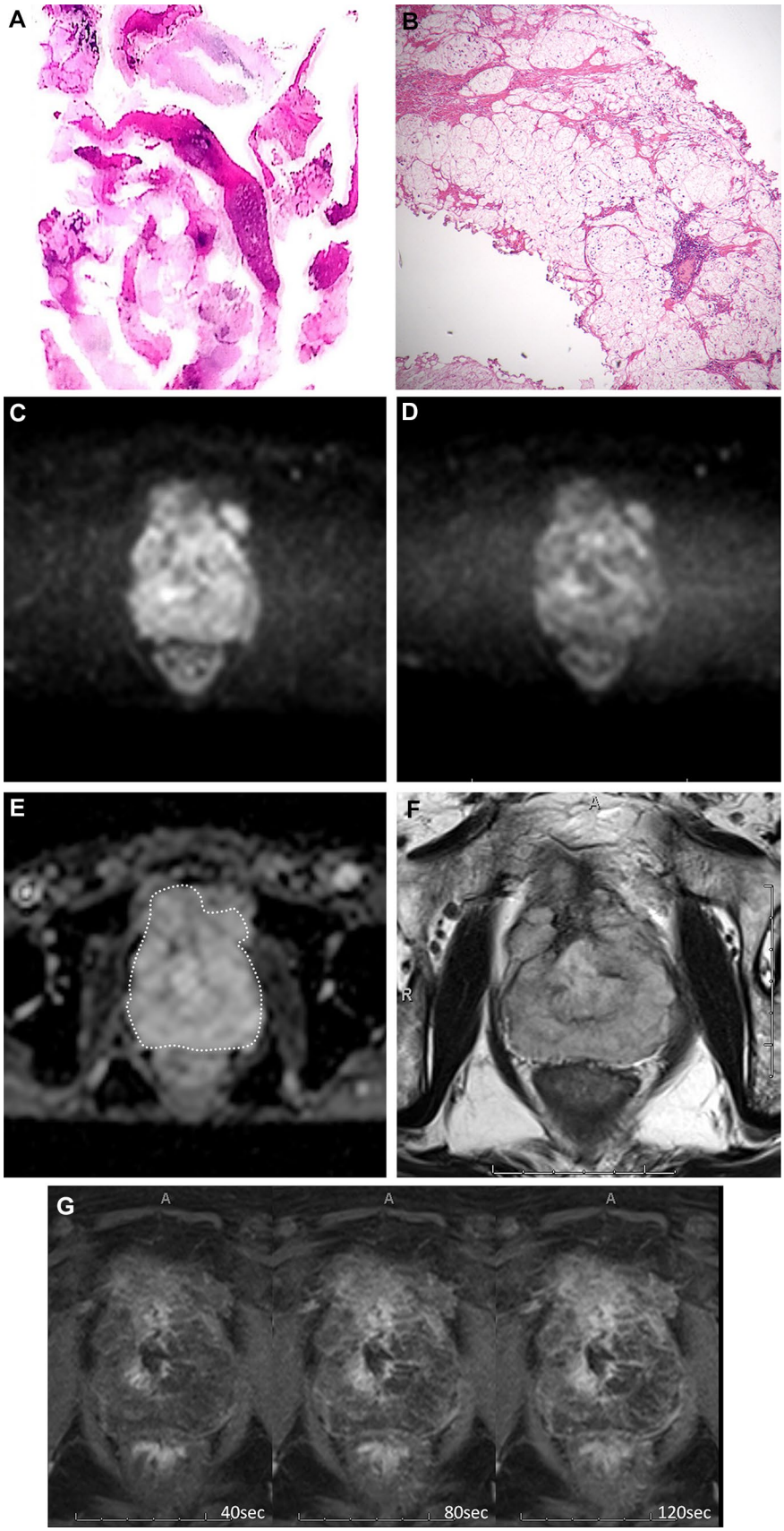

Fig. 3 Case 3: a 75-year-old man with dysuria and repeated urinary retention. **a** Hematoxylin and eosin staining of the transurethral resection gross specimens of the prostate. Most of them consisted of mucinous adenocarcinoma. **b** Microscopic examination (hematoxylin and eosin staining, original ×40) revealed tumor cells interspersed with extremely large amounts of mucin. **c** Diffusion-weighted imaging ($b = 1000$) revealed that the entire prostate was occupied by a large strongly hyperintense mass. **d** On high b-value diffusion-weighted images (b = 1500), the signal of the mass appeared decreased compared with the image with $b = 1000$. **e** The mean apparent diffusion coefficient of the mass was as high as 1.66×10^{-3} mm^2/s. **f** The mass extending well outside the capsule also appeared slightly hyperintense on T2-weighted images, so the hyperintensity on diffusion-weighted images was considered to be caused by T2 shine-through effect. **g** Minimal early enhancement was evident on dynamic contrast-enhanced MRI

Case 4

A 68-year-old man was referred to our hospital with a high PSA (8.15 ng/mL) identified during treatment of diabetes and hypertension. His physical examination, including DRE, was normal. Prostate MRI was performed but there was no obvious lesion on T2WI (Fig. 4a). Scanning was terminated at the request of the patient before DWI or DCE-MRI could be performed. He underwent prostate biopsy 40 days after the MRI and it revealed Gleason score 8 (4 + 4) adenocarcinoma in the right PZ. Radical prostatectomy was performed 67 days after the MRI, assuming a diagnosis of clinical T1cN0M0. Postoperative pathology revealed Gleason score 7 (4 + 3) mucinous adenocarcinoma measuring 2.0 × 1.5 cm in the right PZ with extra-prostatic extension and perineural invasion (Fig. 4b, c). The surgical margin was negative. The specimen's histological stage was T3a. His follow-up is ongoing without any signs of recurrence for 45 months.

Discussion

Mucinous adenocarcinoma of the prostate is a rare variant of prostate carcinoma that is characterized by pools of extracellular mucin. Outcome and prognostic significance of mucinous adenocarcinoma are disputable and not fully understood. Although mucinous adenocarcinoma was previously accepted as an aggressive disease, a newly published series demonstrated that it had a comparable, if not more favorable, prognosis [4]. Because of its rarity and conflicting reports regarding the behavior of the disease, the optimal treatment strategy is not clear. Most series report the efficacy of surgery [6].

Although there have been only a very few reports about MRI findings of mucinous adenocarcinoma of the prostate, some of them have stated that it poses more diagnostic difficulties on MRI than common adenocarcinoma. There are two reasons for this: (1) mucinous adenocarcinoma appears hyperintense on T2WI, reflecting its large extracellular mucin content, and lesions localized in the PZ tend to be isointense to the surrounding tissue; and (2) it does

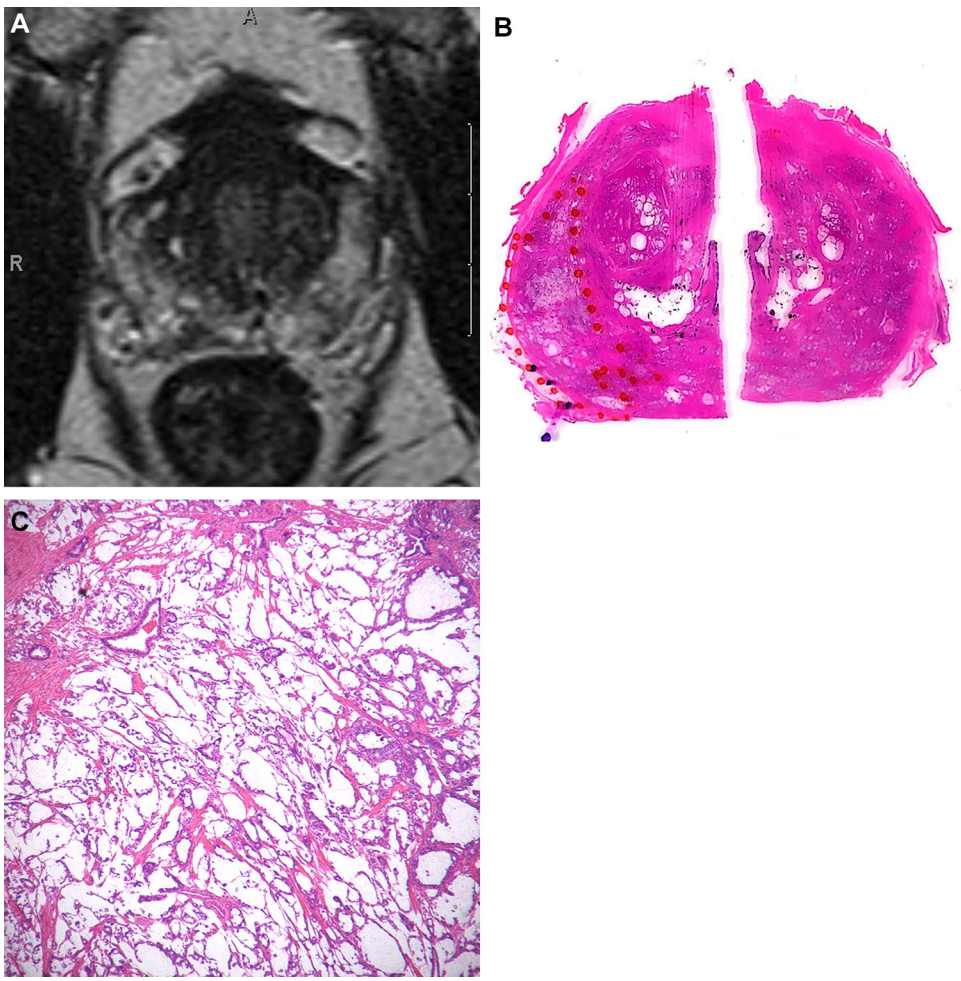

Fig. 4 Case 4: a 68-year-old man with high PSA (8.15 ng/mL). **a** On T2-weighted images, the lesion was isointense to the surrounding PZ, making the lesion difficult to be distinguished. **b** Hematoxylin and eosin staining of a gross specimen revealed a tumor in the right PZ (outlined). **c** Microscopic examination (hematoxylin and eosin staining, original × 40) revealed mucinous adenocarcinoma with high extracellular mucin content

not exhibit the low citrate peak and high choline peak on MR spectroscopy that are characteristic of common prostate adenocarcinoma [3, 4].

In our four cases, we also observed that all lesions appeared hyperintense on T2WI. In one case (Case 2), the lesion contained two components with different intensities, one of which was comparatively hypointense. The two lesions localized in the PZ (Cases 1 and 4) were isointense with the surrounding normal PZ and were difficult to identify on T2WI. In all three patients who underwent DWI, the lesion appeared hyperintense on $b = 1000$ DWI. However, the signal reduction on higher b-value DWI ($b = 1500$ or 2000) was significant especially in cases 2 and 3, and the contrast with the surrounding normal tissue was decreased in case 2. DWI with $b = 1000$ was more useful than DWI with higher b-value in this case. ADC was either high or only slightly decreased, with values of $1.02–1.66 \times 10^{-3}$ mm^2/s, unlike common prostate adenocarcinoma. Therefore, the hyperintensity on DWI was attributed to the T2 shine-through effect. Early enhancement was observed in two of the three patients who underwent DCE-MRI (Cases 1 and 2; in Case 2 early enhancement was only present in the hypointense area on T2WI), and gradual enhancement was identified in the other patient (Case 3). The contrast patterns in the three patients undergoing DCE-MRI study showed no common features.

We speculate that these imaging features may reflect pathological findings such as the proportion of the components represented by extracellular mucin, and the cell density. In breast cancer, mucinous carcinoma has a significantly higher ADC compared with those of other types of cancer and benign tumors, and ADC is reportedly negatively correlated with cell density [7]. Pure mucinous carcinoma of the breast, which typically has a low cell density, is known to exhibit gradual enhancement in DCE-MRI; and this is believed to be due to the gradual spread of contrast agent through the highly mucinous interstitium. However, pure mucinous carcinomas with high cell density are known to exhibit early enhancement [8]. The comparatively low ADC and early enhancement were evident in Case 1, a patient whose lesion contained scattered areas of high cell density with a relatively low extracellular mucin content, whereas the ADC was highest and gradual enhancement was evident in Case 3, a patient whose lesion had an extremely high extracellular mucin content and a low cell density. These observations were not contradictory to the findings previously reported in breast mucinous carcinomas.

In all four cases, mucinous adenocarcinoma exhibited very different MRI features from those of usual prostate adenocarcinoma, in which the tumor is hypointense on T2WI, has a lower ADC value, and exhibits early enhancement in DCE-MRI. In addition, hyperintensity on DWI was attributed to the T2 shine-through effect in mucinous adenocarcinoma, whereas it is known to be due to diffusion restriction in common adenocarcinoma [5]. The diagnosis of mucinous adenocarcinoma could be difficult when using PI-RADS v2, which is based on imaging features of common prostate carcinoma. Among the cases, Case 1 and 3 could not be well classified according to PI-RADS v2, and Case 2 was classified as Category 2. When interpreting MRI of the prostate according to PI-RADS v2, it is necessary to be aware that such rare exceptional cancers may exist.

Conclusion

We reported the MRI findings in four patients with mucinous adenocarcinoma of the prostate. The lesions appeared hyperintense on T2WI and DWI ($b = 1000$), but there was little or no decrease in ADC.

MRI findings in mucinous adenocarcinoma are very different from those in the common type of prostate adenocarcinoma. The conventional PI-RADS v2 interpretation method is not suitable for mucinous adenocarcinoma. Those who interpret prostate MRI should be aware of this rare and unique subtype of prostate cancer.

Acknowledgements We are grateful to Prof. Manabu Minami for valuable advice.

Funding No funding for the present study was received from any companies or organizations.

Compliance with ethical standards

Conflict of interest No authors have any conflict of interest related to this manuscript.

References

1. Humphrey P, Amin MB, Berney D et al. (2016) Acinar adenocarcinoma. In Moch H, Humphrey PA, Ulbright T, Reuter VE eds. Pathology and genetics: tumors of the urinary system and male genital organs. WHO classification of tumors. 4th ed. Zurich, Switzerland: IARC Press, 136-150.
2. Epstein JI, Lieberman PH. (1985) Mucinous adenocarcinoma of the prostate gland. Am J Surg Pathol. 9:299-308.
3. Westphalen AC, Coakley FV, Kurhanewicz J, Reed G, Wang ZJ, Simko JP. (2009) Mucinous adenocarcinoma of the prostate: MRI and MR spectroscopy features. AJR Am J Roentgenol. 193(3):W238-43.
4. Li Y, Mongan J, Behr SC, Sud S, Coakley FV, Simko J, Westphalen AC. (2016) Beyond prostate adenocarcinoma: expanding the differential diagnosis in prostate pathologic conditions. Radiographics. 36(4):1055-75.
5. American College of Radiology, MR Prostate Imaging Reporting and Data System version 2.0 2014.

6. Guler OC, Onal C, Erbay G, Bal N. (2014) Prostate mucinous carcinoma treated with definitive radiotherapy and hormonal therapy: case report and review of the literature. Clin Genitourin Cancer 12(2):e43-6.
7. Woodhams R, Kakita S, Hata H, Iwabuchi K, Umeoka S, Mountford CE, Hatabu H. (2009) Diffusion-weighted imaging of mucinous carcinoma of the breast: evaluation of apparent diffusion coefficient and signal intensity in correlation with histologic findings. AJR Am J Roentgenol. 193(1):260-6.
8. Monzawa S, Yokokawa M, Sakuma T, Takao S, Hirokaga K, Hanioka K, Adachi S. (2009) Mucinous carcinoma of the breast: MRI features of pure and mixed forms with histopathologic correlation. AJR Am J Roentgenol. 192(3):W125-31.